ELSEVIER

Contents lists available at ScienceDirect

Chemical Engineering Science

journal homepage: www.elsevier.com/locate/ces



Foliar uptake of biocides: Statistical assessment of compartmental and diffusion-based models

Enrico Sangoi a, Federica Cattani, Faheem Padia c, Federico Galvanin a,*

- ^a Department of Chemical Engineering, University College London, Torrington Place, London, WC1E 7JE, United Kingdom,
- b Process Studies Group, Syngenta, Jealott's Hill International Research Centre, Berkshire, Bracknell, RG42 6EY, United Kingdom,
- ^c Formulation Technology Group, Syngenta, Jealott's Hill International Research Centre, Berkshire, Bracknell, RG42 6EY, United Kingdom,

ARTICLE INFO

Keywords: Model identification Foliar uptake Data augmentation Correlation study Practical identifiability

ABSTRACT

The global population increase leads to a high food demand, and to reach this target products such as pesticides are needed to protect the crops. Research is focusing on the development of new products that can be less harmful to the environment, and mathematical models are tools that can help to understand the mechanism of uptake of pesticides and then guide in the product development phase. This paper applies a systematic methodology to model the foliar uptake of pesticides, to take into account the uncertainties in the experimental data and in the model structure. A comparison between different models is conducted, focusing on the identifiability of model parameters through dynamic sensitivity profiles and correlation analysis. Lastly, data augmentation studies are conducted to exploit the model for the design of experiments and to provide a practical support to future experimental campaigns, paving the way for further application of model-based design of experiments techniques in the context of foliar uptake.

1. Introduction

As the world's population continues to grow and the planet's resources remain limited, ensuring sufficient food production becomes a crucial challenge both in the present and for the coming decades. In tackling this issue, the development of improved and safer biocides will be essential to optimize crop yields and meet the increasing demand for food. This brings forth the need for innovative solutions that align with sustainable agricultural practices (Umetsu and Shirai, 2020).

Crop protection products such as herbicides and pesticides can be delivered to the plants via different methods, with the spraying on the foliage being one of the most relevant ones for field applications. The process that bring the active ingredient (AI) from the mixing tank to the biological target sites is determined by a series of inter-correlated processes in the biodelivery chain. Having a quantitative understanding of these processes and their effect on the product efficacy is fundamental for developing innovative solutions, and mathematical models are tools that can help researchers in this field and guide further experimental directions. While essential for crop protection and beneficial for tackling food demand needs, the use of pesticides raises concerns about environmental impact, particularly in terms of soil and water contamination (Aktar et al., 2009), as well as the impact on global ecosystems (Sharma et al., 2019). This underscores the heightened importance of develop-

ing tools and technologies that can contribute to the production of safer pesticides for the surrounding environment.

Among all the processes identified in the biodelivery chain, the foliar uptake of the AI (Franke, 1967), i.e. the process of absorption of the AI through the leaves (Fernández et al., 2021), is not completely understood and influenced by several factors, while being a crucial step in the path that leads the AI from the tank to the target sites, i.e. the biological macromolecules essential for the physiological functions of pests, weeds, and pathogens, that interact with the biocide (Zhang et al., 2025). Therefore more effort both theoretical and experimental is needed to characterize this phenomenon subject to high uncertainty in its description.

Several works can be found in literature tackling the question of how to describe the foliar uptake process. The models available in the literature can be divided in three categories (Trapp, 2004): *i*) empirical correlations, *ii*) compartmental models, and *iii*) diffusion-based models. Examples of empirical correlations can be found in Briggs et al. (1987) and Forster et al. (2004), however these models are unable to describe the underlying mechanism. Compartmental models have been applied to physiological systems for several decades (Rowland et al., 1973), with specific applications also to foliar uptake, e.g. in the works by Bridges and Farrington (1974); Satchivi et al. (2000) and Fantke et al. (2013). Some works in literature (Schreiber, 2006) suggest that the process of AI uptake through the cuticle, i.e. the outermost layer of leaves, can be

E-mail address: f.galvanin@ucl.ac.uk (F. Galvanin).

^{*} Corresponding author.

by diffusion. Starting from this consideration, diffusion-based mechanistic models have been proposed in literature for the characterization of foliar uptake, e.g. in Mercer (2007) and Tredenick et al. (2017). Other models for plant uptake (Li, 2025) include, along with foliar uptake, also the description of other processes such as root uptake and/or uptake through the skin of fruits, however, the focus of this paper is solely on the uptake through the leaves. To the best of our knowledge, there is no work proposed in literature where a systematic approach is applied for the development and statistical assessment of foliar uptake models.

The objective of this study is to obtain and statistically validate a predictive model to represent the phenomena occurring within the leaves in a quantitative way. To model biological systems, uncertainty typically arises in the experimental data and in the definition of a suitable structure of the model, i.e. in which phenomena should be included in the mathematical formulation. Since the foliar uptake case study involves biological systems, the large uncertainty in the experimental observations must be taken into consideration when assessing the reliability of the mathematical models in a statistically sound approach.

This paper approaches the problem with a systematic modeling framework presented in Section 2. Different models, described in Section 3, are considered for the characterization of foliar uptake. The results of their comparison are presented in Section 4, focusing on the identifiability of model parameters and data augmentation studies con-

ducted to exploit information from the models for the design of additional experiments. Section 5 summarizes the achievements of this study and points the direction of future works.

2. Methodology

The general modeling framework considered in this study to obtain a reliable predictive model for the characterization of foliar uptake is presented in Fig. 1. The first step in the procedure is to formulate a set of candidate models, which can be based on previous literature available, the understanding of the physico-chemical processes involved in the system and preliminary experimental observations. The general formulation of a dynamic model involving differential and algebraic equations is the following

$$\begin{cases} \dot{\mathbf{x}}(t) = f(\mathbf{x}(t), \mathbf{u}(t), \theta, t) \\ \hat{\mathbf{y}}(t) = g(\mathbf{x}(t), \mathbf{u}(t), \theta, t) \end{cases}$$
(1)

where t is the variable time, $\mathbf{x}(t)$ is a N_x -dimensional vector of system state variables, $\dot{\mathbf{x}}(t)$ the vector of time derivatives, $\mathbf{u}(t)$ the N_u -dimensional vector of known system inputs, $\boldsymbol{\theta}$ the N_{θ} -dimensional vector of model parameters, and $\hat{\mathbf{y}}(t)$ the N_y -dimensional vector of predicted system outputs.

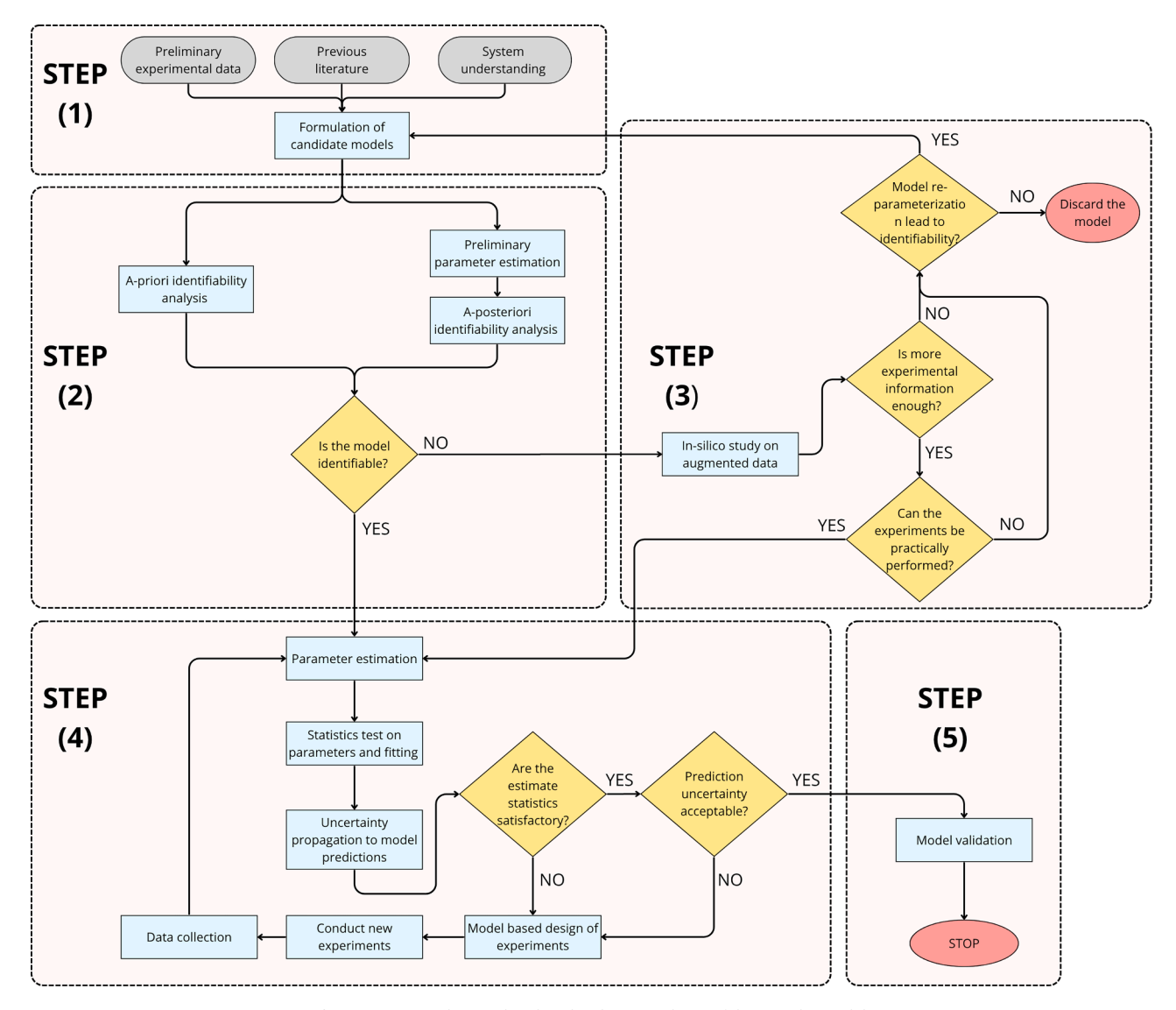


Fig. 1. Framework considered to develop a predictive foliar uptake model.

Once the candidate models are formulated, it is important to test the identifiability of their parameters (step 2 in Fig. 1), i.e. if the model parameters can be uniquely identified from a given set of input and output measurements. Identifiability methods can be distinguished between *a-priori* and *a-posteriori* tests (Miao et al., 2011): *a-priori* methods consider uniquely the structure of the model, while *a-posteriori* techniques start from preliminary experimental data and include practical experimental limitations.

The problem of model identifiability is expressed as

$$\hat{\mathbf{y}}(\theta_1) = \hat{\mathbf{y}}(\theta_2) \Rightarrow \theta_1 = \theta_2,\tag{2}$$

meaning that if the model predictions \hat{y} are identical for some parameter vectors θ_1 and θ_2 , then these vectors must be the same, i.e. $\theta_1 = \theta_2$. If the condition in Eq. (2) does not hold, then the model is not-uniquely identifiable, i.e. there exist two distinct vectors θ_1 and θ_2 which give the same model predictions.

If the model is not identifiable a-posteriori, before discarding it, other questions are posed in the proposed scheme (step 3). The first question is whether having additional experimental observations would be sufficient to solve the identifiability issues. To answer this question, an in silico study is conducted by simulating new experimental data and subsequently evaluating the expected improvement in the statistical quality of the estimates to justify the need for additional data. Moreover, it must be considered that in a real case application experiments will also have to be conducted in practice, which is another important decision block. If the outcome of these decision is still negative, model re-parametrization methods can be considered to solve the identifiability issues before removing a model from the set of candidate ones.

The modeling procedure then continues (step 4) with parameter estimation and statistical tests to assess both the quality of fitting and the precision on parameter estimation. Given that the final objective is to apply the model in practice, the next step is to propagate the uncertainty from parameters to model predictions, to assess whether this uncertainty is within an acceptable range. If the outcome of statistical tests and uncertainty propagation is not satisfactory, model-based design of experiments (MBDoE) can be applied to optimally design additional experiments, and the additional experimental evidence will be used to re-estimate the model parameters (Franceschini and Macchietto, 2008). Finally, the modeling procedure is concluded (step 5) by validating the model on independent experimental observations.

The following subsections will present in detail the methodology employed for testing model identifiability and for the in silico data augmentation study, which are the focus of the results presented in this paper.

2.1. Identifiability analysis

This paper focuses on the study of a-posteriori identifiability to assess whether the parameters can be identified in a practical scenario with real experimental data.

Practical identifiability tests considered in this study are based on the analysis of local sensitivity and correlation matrix since they are less expensive from the computational point of view compared to alternative methods such as Markov Chain Monte Carlo, and their application has been validated in several works available in the literature (Wieland et al., 2021).

2.1.1. Local sensitivity analysis

This analysis is *local* because it is performed around a nominal value for parameters $\hat{\theta}$, which can be estimated from preliminary data. To construct the dynamic sensitivity matrix, $s_{ij}(t_k)$ the sensitivity of the ith response y_i to the jth parameter $\hat{\theta}_j$ at the kth sampling time t_k is calculated as

$$s_{ij}(t_k) = \frac{\partial \hat{y}_i(t_k)}{\partial \hat{\theta}_i} \tag{3}$$

So that the dynamic sensitivity matrix S is obtained

$$S_{N_{y}N_{sp}\times N_{\theta}} = \begin{bmatrix} s_{11}(t_{1}) & \dots & s_{1N_{\theta}}(t_{1}) \\ \vdots & \ddots & \vdots \\ s_{11}(t_{N_{sp}}) & \dots & s_{1N_{\theta}}(t_{N_{sp}}) \\ \vdots & \ddots & \vdots \\ s_{N_{y}1}(t_{1}) & \dots & s_{N_{y}N_{\theta}}(t_{1}) \\ \vdots & \ddots & \vdots \\ s_{N_{y}1}(t_{N_{sp}}) & \dots & s_{N_{y}N_{\theta}}(t_{N_{sp}}) \end{bmatrix}$$

$$(4)$$

where N_{sp} is the number of sampling points and t the N_{sp} -dimensional vector of sampling times.

The dynamic sensitivity is evaluated over the whole time domain and the profiles plotted. If two or more parameters give overlapping profiles, this is an indication of practical non-identifiability, i.e. the corresponding parameters have the same effect on the system response and are correlated.

2.1.2. Correlation matrix method

The correlation matrix approach is used to evaluate the identifiability of parameters, which relies on the matrix of sensitivities S computed in Eq. (4). Given a preliminary estimate of the model parameters $\hat{\theta}$, the matrix S is combined with the variance-covariance matrix of the measurements Σ_y , i.e. a diagonal matrix with the observed variance from experimental replicates on the main diagonal, to calculate the Fisher information matrix H (Walter and Pronzato, 1997) as

$$H = S^T \Sigma_{\gamma}^{-1} S + H^0 \tag{5}$$

where \pmb{H}^0 is the preliminary information on the parameters, which can be neglected if no prior information is available. The variance-covariance of the estimates $\pmb{V}_\theta = \{V_{\theta_{ij}}\}$ is approximated by the inverse of the observed \pmb{H} in the form

$$V_{\alpha} = H^{-1}. \tag{6}$$

The correlation matrix is then defined as $\mathbf{R} = \{r_{ij}\}$, where

$$r_{ij} = \frac{V_{\theta_{ij}}}{\sqrt{V_{\theta_{ii}}V_{\theta_{jj}}}} \quad \forall i, j = 1, \dots, N_{\theta}$$
 (7)

A correlation between parameters higher than 0.99 is a sign of practical non-identifiability, approaching a singular Fisher information matrix (Rodriguez-Fernandez et al., 2006). In this study, a conservative threshold of 0.95 is chosen as critical correlation.

2.2. Data augmentation study

Two studies are performed to evaluate experimental conditions enabling statistically reliable model identification. These studies rely on in silico generated data, where a noise factor is added to the model predictions to reliably reproduce real experimental data. The parameters in the variance model are calibrated on the variance observed experimentally. Both data augmentation procedures are presented in the following subsections.

2.2.1. Single additional sample

The first data augmentation study is performed to assess the expected improvement in the statistics of parameter estimation, data fitting, and identifiability of model parameters deriving from the availability of additional experimental data, depending on the experimental design φ , i.e. the set of conditions at which the new data are collected.

The steps involved in this study are:

- 1. The experimental design vector $\boldsymbol{\varphi}$ is defined as $\{t_1,\dots,t_{N_{new}}\}$, where N_{new} is the number of sampling times under assessment in the design space Φ
- 2. The N_{new} design variables t_i are sampled using an equally spaced sampling of the design space defined by upper and lower bounds on the experimental sampling times.

3. New experimental data are generated in silico from the model for each of the N_{new} elements of the design vector φ , and added to the original dataset ψ_o to obtain N_{new} augmented datasets:

$$\psi_i = \psi_0 + \{\hat{\mathbf{y}}(\mathbf{x}, \mathbf{u}, \hat{\boldsymbol{\theta}}_0, t_i) + \varepsilon_i\} \quad \forall i = 1, \dots, N_{new}$$
 (8)

where $\hat{\theta}_0$ is the preliminary estimate of parameters, and the error $\epsilon_i \in \mathcal{N}(\mathbf{0}, \sigma_i^2)$ is obtained from a normal distribution with zero mean and variance σ_i^2 . The variance is obtained from a heteroscedastic model

$$\sigma_i^2 = \omega^2 (\hat{\mathbf{y}}^2)^{\gamma/2} \tag{9}$$

where parameters ω and γ are calibrated from the variance observed in the original experimental dataset.

4. Perform parameter estimation for every N_{new} augmented dataset ψ_i , and evaluate the statistics on the new estimates. The results are the new estimate θ_i , the covariance of the parameters V_{θ_i} , the FIM H_i , the t-values of the parameters t_{θ_i} (see Eq. (10)) and the sum of squared residuals, i.e. the χ_i^2 statistics, for all $i=1,\ldots,N_{new}$.

$$t_{\theta_j} = \frac{\hat{\theta}_j}{t(\frac{1+\alpha}{2})\sqrt{V_{\theta_{jj}}}} \quad \forall j = 1, \dots, N_{\theta}$$
 (10)

In Eq. (10), the value $t(\frac{1+\alpha}{2})$ is obtained from a Student's distribution with $\dim(\psi) - N_{\theta}$ degrees of freedom and significance $\frac{1+\alpha}{2}$. The *t*-values of the parameters calculated as in Eq. (10) are compared to a t-reference value $t(\alpha)$ given the significance level α .

This first data augmentation study is performed to understand under which conditions, i.e. sampling time, an additional experiment should be conducted so that the new data will carry more information in the modeling process.

2.2.2. Multiple additional samples

The second data augmentation study is performed to verify how many additional data are required to solve parameter identifiability issues, i.e. to estimate the full set of model parameters precisely. The procedure for this second study is the following:

- 1. Select and fix the design space Φ for experimental design variables φ starting from the results of the previous study.
- 2. Select n_{sp} sampling points, i.e. $\varphi_{n_{sp}} = \{t_1, \dots, t_{n_{sp}}\}$, uniformly distributed in the design space Φ .
- 3. Generate new data ψ_{new} in silico for each sampling point in $\varphi_{n_{sn}}$,

$$\psi_{new} = \{ \hat{\mathbf{y}}(\mathbf{x}, \mathbf{u}, \hat{\boldsymbol{\theta}}_0, t_i) + \boldsymbol{\varepsilon}_i \mid t_i \in \boldsymbol{\varphi}_{n_{s_p}} \quad \forall i = 1, \dots, n_{s_p} \}$$
 (11)

where the noise term ε_i is modeled as in Eq. (9).

4. Add the new data ψ_{new} to the original dataset available ψ_o to obtain the augmented dataset ψ_A .

$$\psi_A = \psi_o + \psi_{new} \tag{12}$$

- 5. Perform parameter estimation and evaluate the statistics, i.e. *t*-test on the estimates.
- 6. Increase the number of sampling points and iterate the procedure from point 2., until the maximum budget is reached.

The following section will present the case study on which the modeling framework is applied. i.e. foliar uptake of pesticides, in particular focusing on the models considered to describe the system behavior.

3. Foliar uptake models

In this paper different candidate models are compared for the description of pesticide uptake through the leaves. In particular the two models included in this study are *i*) a diffusion-based model (Sangoi et al., 2024a), and *ii*) a compartmental model (Sangoi et al., 2024b).

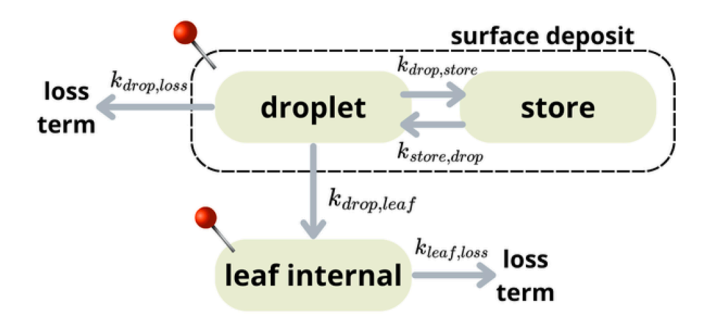


Fig. 2. Graphical representation of the compartmental model for leaf uptake. The pins indicate the observed states, the compartments represent the system states and the arrows the transfer rates between the compartments (model parameters).

3.1. Compartmental model

The compartmental model included in this study to describe the foliar uptake process is presented graphically in Fig. 2, where the pins indicate the observed states in the system. The compartments included in the model formulation are the following: droplet, store, leaf internal, and surface deposit. The droplet is formulated product deposited on the leaf surface, the store compartment contains the active ingredient (AI) crystallized on the surface and not available for uptake, while the surface deposit is the sum of the two compartments, which corresponds to the system state observed experimentally. As for the leaf internal, a single compartment is considered because a more detailed division in the different layers that constitute the leaf would lead to a-priori non-identifiability issues when lacking of experimental observations of the different layers, as observed in a previous study (Sangoi et al., 2024b). Moreover, this choice ensure consistency with the diffusion-based model included in this study to have a fair comparison.

In Fig. 2, the arrows indicate where the mass transfer between the compartments takes place. Mass transfer between the droplet and store compartments is associated to crystallization/solubility processes on the leaf surface (Burkhardt et al., 2012), while the loss term from the droplet takes into account the AI lost, i.e. not available for uptake, due to volatility and/or photo-instability (Bronzato et al., 2023).

The AI in solution in the droplet is available for uptake in the leaf internal compartment $(k_{drop,leaf})$, and then the loss term $k_{leaf,loss}$ takes into account AI consumption inside the leaf due to metabolism or chemical-instabilities which reduce the amount of AI available in the leaf with time.

The mathematical expression of the compartmental model is reported in Eq. (13). The dynamic model is a system of ODEs, which describes the evolution in time of the AI mass in the different compartments.

$$\frac{dm_i}{dt} = \sum_{i \neq i} (k_{ji}m_j - k_{ij}m_i) \tag{13}$$

In Eq. (13), m_i is the mass of AI in compartment i, and k_{ij} the transfer rate of AI from compartment i to compartment j. The $m_i(t)$ values are normalized with respect to $m_{deposit}(t=0)$, therefore transfer rates k_{ij} are expressed in units of min⁻¹.

With respect to the generic formulation presented in Eq. (1), the vector of state variables is $\mathbf{x} := \{m_i\}$, and the vector of model parameters is $\boldsymbol{\theta} := \{k_{ij}\}$. The input in the system is the initial mass in the deposit, $\mathbf{u} = \{m_{dep}(t_0)\}$. The vector of observable outputs is $\mathbf{y} := \{m_{deposit}, m_{leaf}\}$, where $m_{deposit} = m_{droplet} + m_{store}$. The experimental design vector is defined by the sampling times $\boldsymbol{\varphi} = \{t_1, \dots, t_{N_{sp}}\}$.

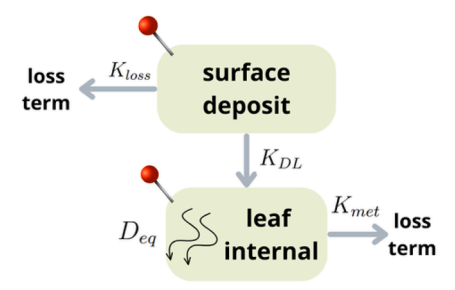


Fig. 3. Graphical representation of the diffusion-based model for leaf uptake: system geometry and key parameters involved. The pins indicate the observed states

3.2. Diffusion-based model

A second model considered in this study is a diffusion-based model. The geometry of the system and the physical phenomena included in its mathematical formulation are presented graphically in Fig. 3. Previous studies in the literature (Schreiber, 2006) suggest that the transport mechanism of pesticides through the cuticle, i.e. the external layer in the leaf structure protecting the cellular tissue from the external environment, can be assumed as diffusion. Although, separating the cuticle from the rest of the leaf is extremely complex and time consuming, therefore measuring the uptake in the cuticle and leaf tissue separately is not an activity typically performed in routine biokinetic experimental procedures of foliar uptake of AIs. Since the purpose of this project is to validate a model that can be combined with the in vitro and in vivo experimental campaigns for the development of new biocides, in this diffusion-based model it is assumed that the leaf internal is a homogeneous structure where equivalent diffusion takes place, in the same way that only a single leaf internal compartment is included in the compartmental model presented in Section 3.1.

The system geometry is then divided in two regions, as depicted in Fig. 3: the deposit on the surface and the leaf internal. The physical phenomena included in the model are: equilibrium at the interface between deposit and leaf, diffusion of AI through the leaf, loss from the deposit due to volatility and chemical instability of AI, and consumption of AI in the leaf due to metabolism.

The following equations are included in the general mathematical formulation developed to describe the dynamics of AI uptake from the deposit to the leaf internal region.

$$m_{dep}(t) = C_{dep}(t) \cdot V_{dep}(t) \tag{14}$$

$$\frac{dV_{dep}(t)}{dt} = -K_{evap} \cdot f(V_{dep}) \tag{15}$$

subject to

$$f(V_{dep}) = \begin{cases} 1 & \text{if } V_{dep} > V_{min}, \\ 0 & \text{if } V_{dep} \le V_{min}. \end{cases}$$
 (16)

$$\frac{dC_{dep}}{dt} = -\frac{f(V_{dep})}{V_{dep}} \frac{dV_{dep}}{dt} C_{dep} - K_{loss} C_{dep}$$
(17)

$$K_{DL} = \frac{C_{leaf}(0,t)}{C_{dep}(t)} \tag{18} \label{eq:KDL}$$

$$\frac{\partial C_{leaf}(z,t)}{\partial t} = D_{eq} \frac{\partial^2 C_{leaf}(z,t)}{\partial z^2} - K_{met} C_{leaf}(z,t) - K_{trans}$$
 (19)

$$C_{leaf,tot}(t) = \frac{1}{L_{leaf}} \int_{z=0}^{L_{leaf}} C_{leaf}(z,t) dz$$
 (20)

$$m_{leaf}(t) = C_{leaf,tot}(t) \cdot V_{leaf} \tag{21} \label{eq:21}$$

In the equations reported above, the state variables are the mass of AI in the deposit m_{dep} , the concentration of AI in the deposit C_{dep} , the concentration of AI inside the leaf discretized in space $C_{leaf}(z,t)$, the total concentration of AI inside the leaf $C_{leaf,tot}$, the mass of AI inside the leaf m_{leaf} . The parameters in the model are the evaporation rate K_{evap} , the accounting for losses from the deposit K_{loss} , the partition coefficient for AI between deposit and leaf K_{DL} , the diffusion coefficient inside the leaf D_{eq} , the metabolism rate K_{met} , the translocation to other parts of the leaf/plant K_{trans} . With respect to the generic formulation presented in Eq. (1), the vector of state variables is $x := \{m_{dep}, C_{dep}, m_{leaf}, C_{leaf,tot}\}$, and the vector of model parameters is $\theta := \{K_{evap}, K_{loss}, K_{DL}, D_{eq}, K_{met}, K_{trans}\}$. The input in the system is the initial mass in the deposit, $u = \{m_{dep}(t_0)\}$. The vector of observable outputs is $y := \{m_{dep}, m_{leaf}\}$. The experimental design vector is defined by the sampling times $\varphi = \{t_1, \dots, t_{N_{sp}}\}$.

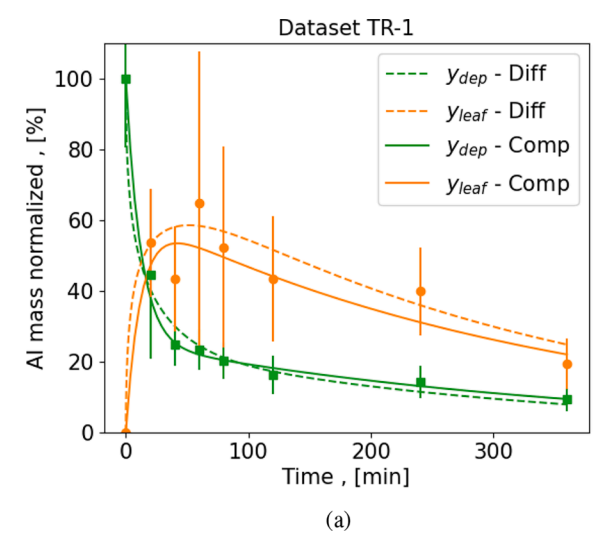
With respect to the compartmental model, the main change is in how the physics of uptake is described. Instead of mass transfer with asymptotic equilibration as described by the k_{ij} parameters of the compartmental model, we now consider instantaneous partitioning at the deposit-leaf interface and diffusion through the leaf, i.e., K_{DL} and D_{eq} . Similarly to the compartmental model, also for the diffusion model the state variables are normalized with respect to the initial amount of AI in the deposit.

Eqs. (14)–(17) describe the dynamics in the deposit on the leaf surface. Eq. (18) relates the concentration of AI in the deposit to the concentration in the leaf at the interface, assuming equilibrium conditions at all times within a boundary layer at the interface between leaf and droplet. In Eq. (18), $C_{leaf}(0,t)$ indicates the concentration of AI at the interface on the leaf side at time t. Eqs. (19)–(21) describe the dynamics in the leaf tissue. The leaf internal region is modeled as a homogeneous structure where diffusion and metabolic consumption take place uniformly throughout the spatial domain.

4. Results and discussion

The analyses on the compartmental and diffusion-based models presented in Section 3 are conducted starting from experimental data of foliar uptake provided by Syngenta. The same procedure and analyses are conducted on two different datasets, named as TR-1 (treatment 1) and TR-2 (treatment 2). The experimental data represent biokinetic experiments of foliar uptake, where the formulated active ingredient (AI) is sprayed on the leaves in a controlled lab environment. Two quantities are measured for each sampling time: the amount of AI left on the leaf surface (i.e. deposit), and the amount of AI inside the leaf (i.e. leaf extract). The two measurements at time t^* are obtained in the following way: firstly, t^* minutes after the product is sprayed on the leaves. these are washed with a solvent to recover the AI on their surface. Secondly, the leaves are macerated and washed with another solvent to recover the AI inside the leaf. The collected samples are analyzed with HPLC to quantify the mass of AI recovered. Since these experiments are destructive for the leaf, experimental replicates must be obtained from different leaves. For each dataset 8 sampling times from the application of the product on the leaf are considered, ranging from 0 to 360 min. Datasets TR-1 and TR-2 are shown in Fig. 4 through the data points and the 95% confidence intervals in the experimental replicates. The two dataset differ for the treatment depending if the leaves are subject to the solar radiation or not, while the combination of AI, formulation and crop are the same for the two treatments considered here.

The results of the analyses are presented with this structure: i) parameter estimation, data fitting and statistical tests (Section 4.1), ii) model identifiability tests (Section 4.2), iii) data augmentation study (Section 4.3). The models have been implemented in python, using the following packages to conduct the study: *pandas* for data manipulation (McKinney et al., 2010), *numpy* for linear algebra routines (Harris et al., 2020), and *scipy* for scientific computing (Virtanen et al., 2020), i.e. for parameter optimization and for calculating t- and χ^2 - statistics.



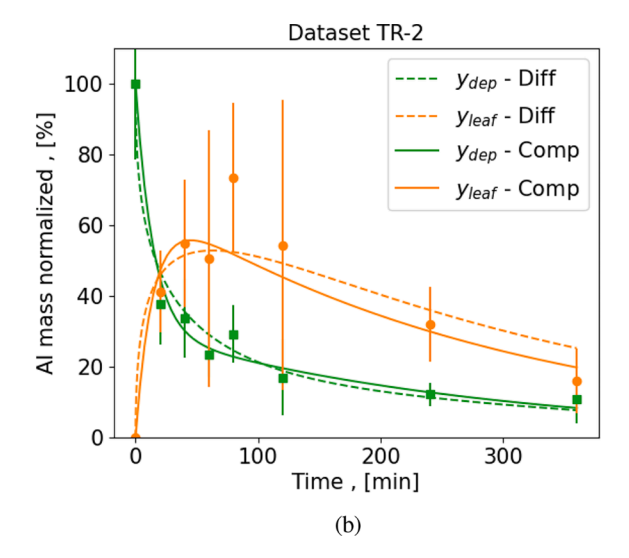


Fig. 4. Fitting of experimental data with the compartmental model (solid line) and diffusion-based model (dashed line). Results for (a) dataset TR-1 and (b) dataset TR-2. Green squares refer to measurements of the deposit on the leaf surface, orange circles to measurement in the leaf tissue.

Table 1Parameter estimates and 95% confidence intervals for the compartmental and diffusion-based models obtained for the datasets TR-1 and TR-2.

Model	Dataset Parameter		Estimate	± 95 % C.I.	Units
Compartmental	TR-1	$k_{drop,store}$	0.01938	± 0.01593	1/min
Compartmental	TR-1	$k_{store,drop}$	0.00363	± 0.00195	1/min
Compartmental	TR-1	$k_{drop,leaf}$	0.05004	+ 0.01390	1/min
Compartmental	TR-1	$k_{drop,loss}$	0.01246	+ 0.00779	1/min
Compartmental	TR-1	k _{leaf,loss}	0.00382	± 0.00072	1/min
		reaj ,toss			
Compartmental	TR-2	$k_{drop,store}$	0.01863	± 0.01456	1/min
Compartmental	TR-2	$k_{store,drop}$	0.00497	± 0.00312	1/min
Compartmental	TR-2	$k_{drop,leaf}$	0.04578	± 0.01819	1/min
Compartmental	TR-2	$k_{drop,loss}$	0.00455	± 0.01112	1/min
Compartmental	TR-2	$k_{leaf,loss}$	0.00483	$\pm~0.00176$	1/min
Diffusion-based	TR-1	D_{eq}	8.012 e-13	± 6.508 e-13	m ² /s
Diffusion-based	TR-1	K_{DL}	1.109 e+01	$\pm 4.618 e + 00$	_
Diffusion-based	TR-1	k_{met}	3.252 e-02	$\pm 4.122 e-02$	1/s
Diffusion-based	TR-1	k_{loss}	2.609 e-02	± 1.011 e-01	1/s
Diffusion-based	TR-2	D_{eq}	4.481 e-13	± 4.631 e-13	m ² /s
Diffusion-based	TR-2	K_{DL}	1.125 e + 01	$\pm 6.458 e + 00$	_
Diffusion-based	TR-2	k_{met}	2.852 e-02	± 3.814 e-02	1/s
Diffusion-based	TR-2	k_{loss}	3.562 e-02	± 7.958 e-02	1/s

4.1. Parameter estimation, data fitting and statistical tests

The parameter estimation results (Table 1) are given in terms of estimated values and 95% confidence intervals obtained after a loglikelihood parameter estimation has been carried out, for both the datasets TR-1 and TR-2. For the diffusion-based model the estimated parameters are K_{DL} , D_{eq} , K_{met} and K_{loss} , assuming the other parameters negligible by setting their value to 0. In particular, for the specific foliar treatment considered in this study, translocation (parameter K_{trans}) to other parts of the plant was not observed experimentally, and K_{evap} is neglected to keep consistency between the compartmental and diffusion-based model. Should these processes be observed, an independent measure of their characteristic parameters can be included in the model as extra loss terms. For both models it is noted that the estimated values of the corresponding model parameters do not change significantly between TR-1 and TR-2, especially when considering the parametric uncertainty. A difference is noted in the compartmental model for the parameter $k_{drop,loss}$, where the absence of UV radiation in TR-2 leads to a lower value of this parameter, however this difference is still within the 95 % confidence intervals. Conversely, for the diffusion-based

Table 2 Quality of data fitting assessed comparing the sum of squared residuals (SSR) to the χ^2 -reference values at 0.05 and 0.95 significance.

Dataset	Model	SSR	$\chi^{2}_{0.05}$	$\chi^{2}_{0.95}$	Test result
TR-1	Compartmental	6.558	4.575	19.675	Passed
TR-1	Diffusion-based	12.835	5.226	21.023	Passed
TR-2	Compartmental	11.343	4.575	19.675	Passed
TR-2	Diffusion-based	16.603	5.226	21.023	Passed

model the estimate of K_{loss} is higher with TR-2 than with TR-1, but these values have an uncertainty region larger than the estimate itself, which do not allow to draw sensible conclusions at this stage.

It must be highlighted that the uncertainty on the estimates is large, in particular for parameters K_{met} and K_{loss} in the diffusion based model.

The predicted profiles after parameter estimation with the compartmental and diffusion-based models are shown in Fig. 4, along with the experimental data used to calibrate the model parameters. The error bars show the 95% uncertainty region in the experimental data. It is observed that both models capture well the AI uptake profiles observed experimentally, as also confirmed by the parity plots in Fig. 5 which compare experimental data with model predictions.

4.1.1. Statistical tests

The data fitting results are reported in Table 2. The sum of squared residuals (SSR) shows that the compartmental model has a better fitting than the diffusion model, since the SSR values obtained with the compartmental model are lower with both datasets. The table reports also the results of the χ^2 -test performed to evaluate the quality of data fitting. The results of the statistical test show that both models provide an adequate fitting of the data since the SSR is between $\chi^2_{0.05}$ and $\chi^2_{0.95}$ both when calibrated on dataset TR-1 and TR-2.

The statistical quality of the estimates is evaluated by means of a t-test, which results are shown in Fig. 6. The compartmental model results (Fig. 6a) depict that the parameter $k_{leaf,loss}$, representing a consumption term inside the leaf, is estimated with a good confidence from both TR-1 and TR-2 datasets, being the t-values higher than the reference t_{ref} . For $k_{drop,leaf}$ the estimate is satisfactory only when the dataset TR-2 is used, while the t-values of all the other parameters are clearly lower than the reference. In particular, the loss term from the droplet $k_{drop,loss}$ is the most critical parameter to estimate, as underlined by the least confidence in the estimate.

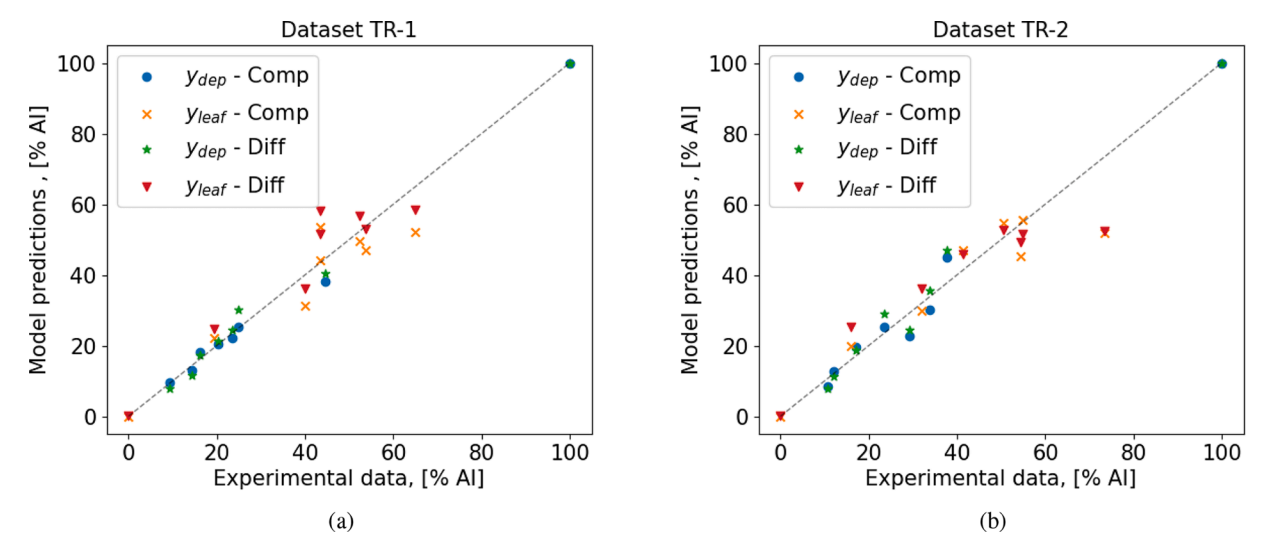


Fig. 5. Parity plots showing the comparison between the experimental data and model predictions for the datasets (a) TR-1 and (b) TR-2. Legend: blue circle - compartmental model, surface deposit; yellow cross - compartmental model, leaf internal; green star - diffusion model, surface deposit; red triangle - diffusion model, leaf internal.

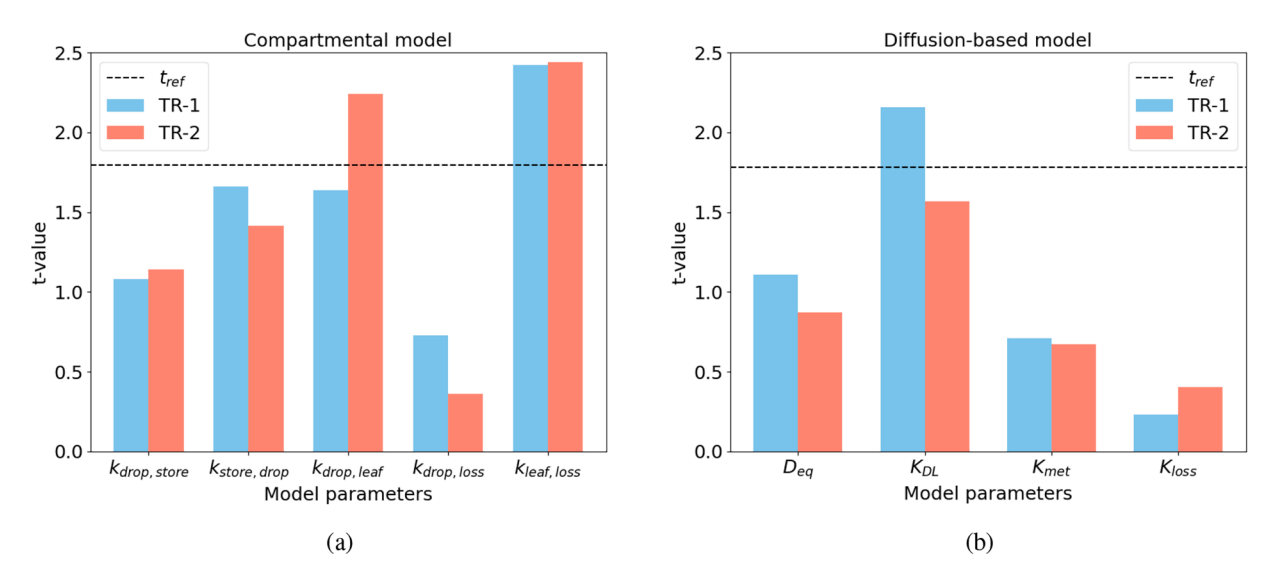


Fig. 6. Bar chart with the values of the *t*-test statistics obtained on datasets TR-1 and TR-2 for (a) the compartmental model and (b) the diffusion-based model parameters.

The t-test results obtained with the diffusion-based model are shown in Fig. 6b. In this case, parameter K_{met} , that describes the AI consumption inside the leaf, and K_{loss} , which represents the loss from the deposit, are both poorly estimated, especially the latter which is the most critical to estimate also for the diffusion-based model. This result goes along with the large variances observed in Table 1. On the other hand, the estimate of the partition coefficient K_{DL} is statistically significant at least with dataset TR-1, while the t-values obtained for D_{eq} are lower than the reference value, therefore its estimate has low confidence from the statistical point of view.

4.2. Model identifiability

To answer the question whether the results on the estimates could be improved by designing new and more informative experiments, the framework presented in the methodology, Section 2 (Fig. 1), is followed. The first analysis conducted is to assess the identifiability of the model parameters by analyzing the dynamic sensitivity profiles, which indicate the impact of the parameters on the output variables in time, then followed by the correlation analysis between the parameters.

4.2.1. Local sensitivity profiles

Results from the sensitivity analysis are shown in Fig. 7 for the compartmental model and Fig. 8 for the diffusion model. This is a local analysis performed around the preliminary estimate of the parameters, and for both models the results are reported starting from the estimate obtained with TR-1 and TR-2. It is observed that the profiles obtained for a given model with the two datasets are similar in their features, so only the profiles for TR-1 will be commented for the sake of conciseness. The profiles for TR-2 are reported in Appendix A in the supplementary material. The values of sensitivity have been normalized for each parameter in the range between -1.0 and +1.0 to show which output measurement has the higher impact for a given parameter.

For the compartmental model it emerges that parameters $k_{drop,store}$ and $k_{store,drop}$ are mostly linked to the measurement on the deposit (Fig. 7a), $k_{leaf,loss}$ depends uniquely on the leaf extract measurement (Fig. 7b), while both outputs are sensitive to the remaining two

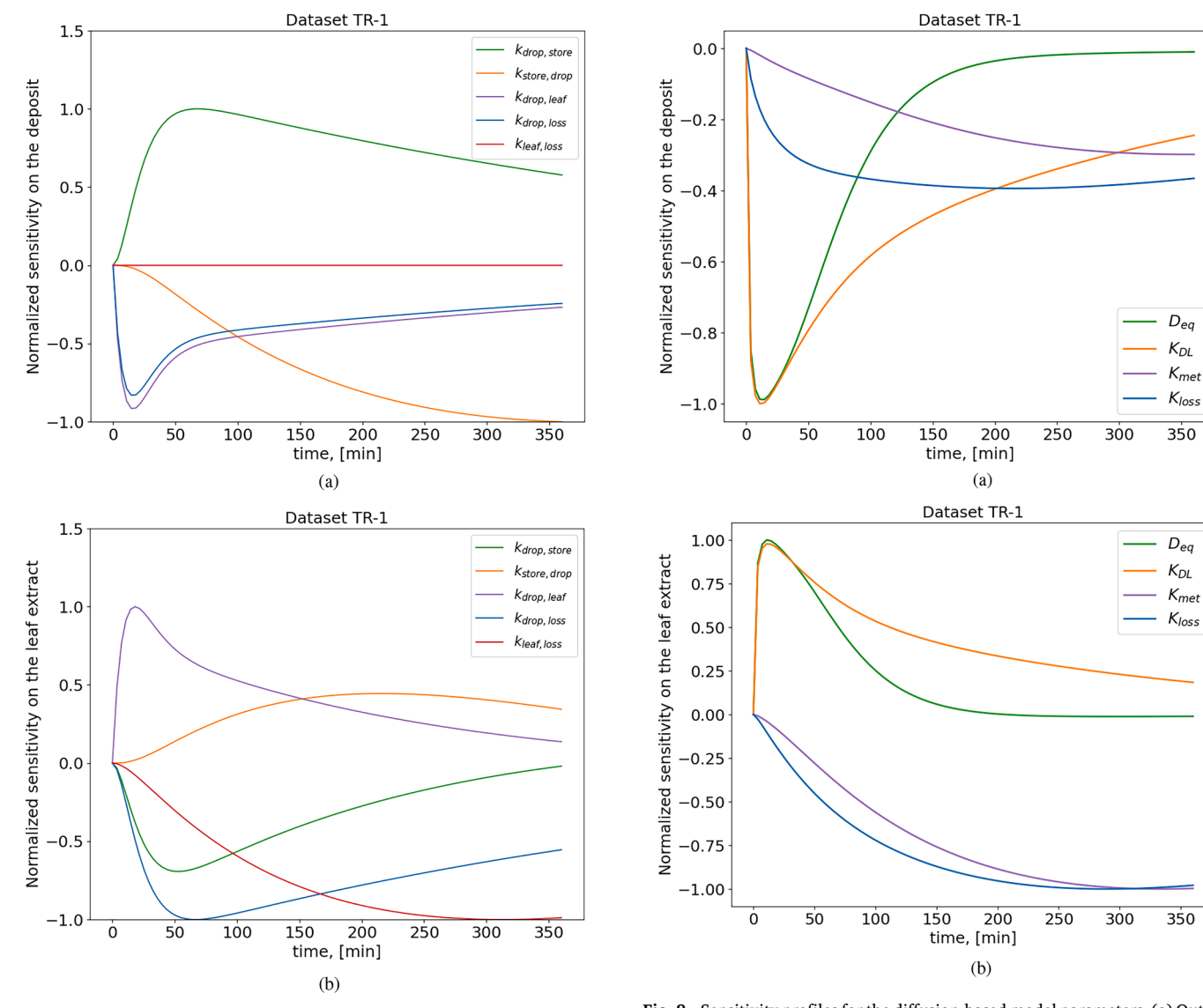


Fig. 7. Sensitivity profiles for the compartmental model parameters. (a) Output: deposit, dataset TR-1; (b) output: leaf extract, dataset TR-1.

Fig. 8. Sensitivity profiles for the diffusion-based model parameters. (a) Output: deposit, dataset TR-1; (b) output: leaf extract, dataset TR-1.

parameters $k_{drop,leaf}$ and $k_{drop,loss}$. It must also be highlighted that the loss due to AI consumption in the leaf ($k_{leaf,loss}$) has the peak of sensitivity between 3 and 6 h since the deposition of the droplet on the leaves, while impact on the measured outputs of the parameters $k_{drop,store}$, $k_{drop,leaf}$ and $k_{drop,loss}$ is stronger in the short time from the deposition (within 1 h), when the initial uptake dynamics takes place.

The sensitivity profiles obtained with the diffusion model are reported in Fig. 8. Also in this case it is observed that the metabolic rate is mostly linked to the leaf extract output (Fig. 8b), and that its effect peaks between 3 and 6 h after the deposition of the formulation on the leaves, similarly to what has been observed with $k_{leaf,loss}$ in the compartmental model. The dependence of K_{loss} on the leaf measurement is very similar to the metabolism rate K_{met} , being the two profiles almost overlapping, but a difference between the two parameters is observed in the deposit (Fig. 8a), which should allow decoupling the effect of these two parameters. The other two parameters K_{DL} and D_{eq} impact both outputs equally at the beginning, and their peak is observed in the first hour from the deposition of the droplets. However, after two hours from the deposition the effect of D_{eq} rapidly drops to zero, while the equilibrium at the interface K_{DL} still holds a significative role in the system dynamics.

4.2.2. Parameter correlation analysis

Practical identifiability issues did not clearly emerge from the dynamic sensitivity profiles, and to confirm this observation, practical identifiability is further tested by studying the correlation between model parameters, following the methodology presented in Section 2. The results of this analysis are reported in Fig. 9 by means of correlation matrices, respectively for compartmental model (Fig. 9a, b) and diffusion model (Fig. 9c, d). Similar results are obtained when conducting the analysis starting with different sets of preliminary data, i.e. TR-1 and TR-2, for a given model among the candidates.

For the compartmental model, the matrix in Fig. 9a and b show a block diagonal trend where $k_{leaf,loss}$ is slightly correlated to $k_{drop,loss}$, while the other three parameters $k_{drop,store}$, $k_{store,drop}$ and $k_{drop,leaf}$ are moderately inter-correlated. However, the maximum correlation index observed between pairs of parameters in the compartmental model is 0.91 (for $k_{drop,store}$ and $k_{drop,leaf}$), which is below the conservative threshold of 0.95 defined in the methodology. Therefore, the analysis tells that practical identifiability is not an issue for the compartmental model parameters, whose estimates could then be improved by providing additional data from properly designed foliar uptake experiments.

The correlation matrix of the diffusion model parameters in Fig. 9c and d suggests that parameters K_{met} and K_{loss} could potentially have

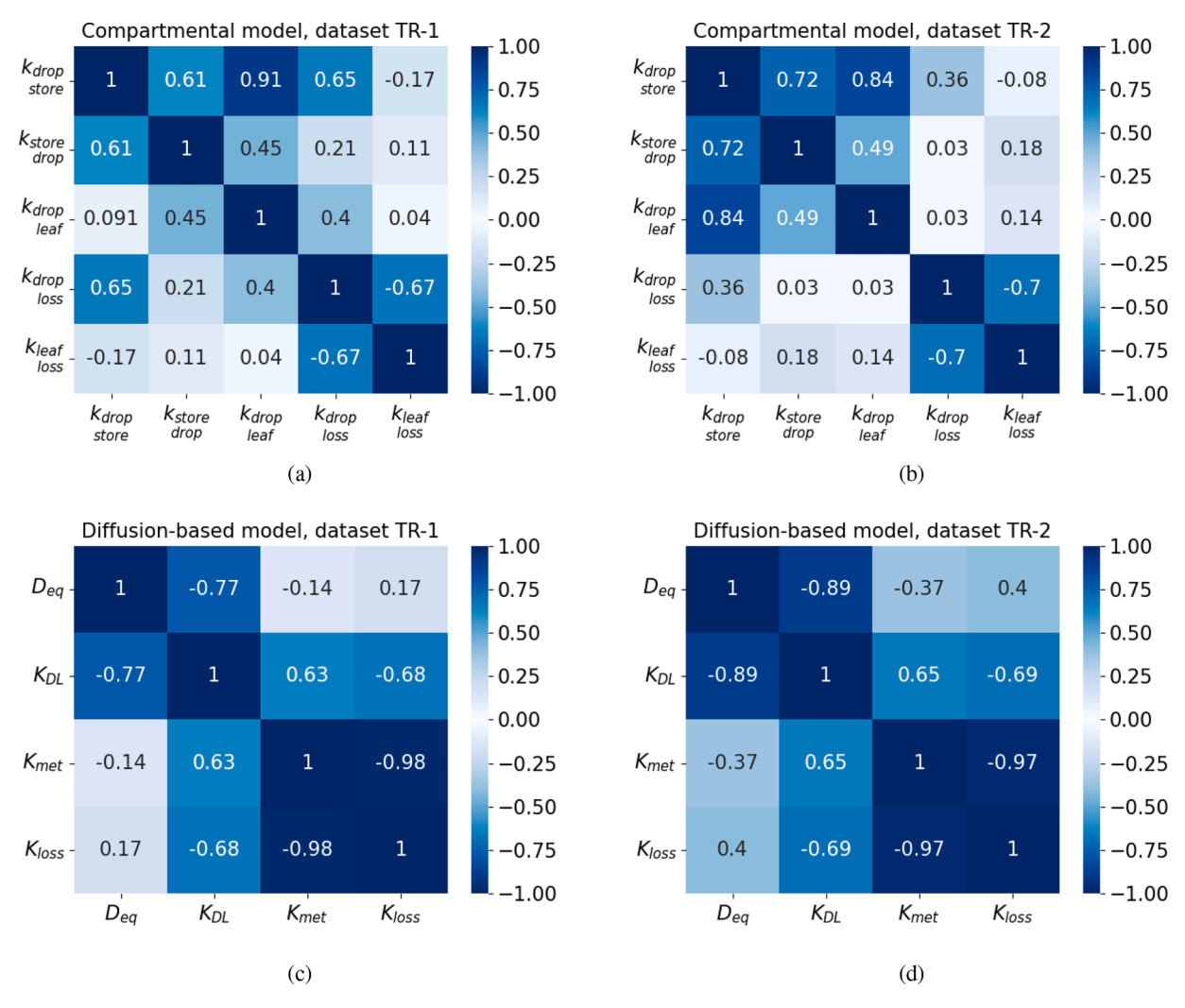


Fig. 9. Correlation matrix for the model parameters: (a) compartmental model, dataset TR-1; (b) compartmental model, dataset TR-2; (c) diffusion-based model, dataset TR-1; (a) diffusion-based model, dataset TR-2.

identifiability problems since the observed correlation index between the two parameters is -0.98, exceeding the conservative threshold of 0.95. The parameters D_{eq} and K_{DL} have a correlation of -0.77 and -0.89 in the two cases, noting that the difference is due to the local nature of the analysis, conducted around the local estimate of the parameters. In any case, for these two parameters signs of identifiability issues did not emerge, also when looking at their correlation with K_{met} and/or K_{loss} .

4.3. Data augmentation

Following the procedure presented in the methodological framework, the last analysis presented in this paper is the data augmentation study. The two different data augmentation strategies described in the methodology Section 2.2 are presented:

- Strategy 1 single additional sample. Study conducted to assess the expected improvement in parameter estimation identifiability depending on the experimental design φ , i.e. sampling time in this case.
- Strategy 2 multiple additional samples.
 Analysis to verify how many additional data are required to solve parameter identifiability issues.

Results from the two different augmentation strategies are reported in the following subsections.

4.3.1. First augmented data study

The first analysis considers the effect of adding one additional experimental data to the 8 data points in the original dataset to assess the expected improvement in the statistics of parameter estimation, data fitting and identifiability of model parameters. In this study, the impact of the different location in time for the additional sample is evaluated. The noise factor added to the simulated measurement is generated with a heteroscedastic model calibrated on the noise observed in the original dataset, to replicate the data variability of the real experiments. This study is conducted on both available datasets TR-1 and TR-2, and the heteroscedastic model is calibrated independently for each case.

Results are shown in Fig. 10 for the compartmental model and TR-1 and Fig. 11 for the diffusion model and TR-1. The results obtained with dataset TR-2 are available in the supplementary material - Appendix B. For each combination of model and dataset the following plots are reported: (a) the whole set of additional experimental data simulated, and the profiles with respect to the sampling time of the additional data point of (b) $\log_{10}(\det(FIM))$, (c) the *t*-value statistics for the parameters, (d) the standard deviation of the estimates, (e) the SSR with the χ^2 reference values. Dashed lines in the plots indicate the initial values obtained with the original dataset before adding the new simulated data point.

The profiles of the determinant of the FIM depict oscillations around the initial value for the compartmental model. This can be due to the high variability in experimental noise added to the new data, which is included in the calculation of FIM in the term Σ_{ν} as per Eq. (5), and

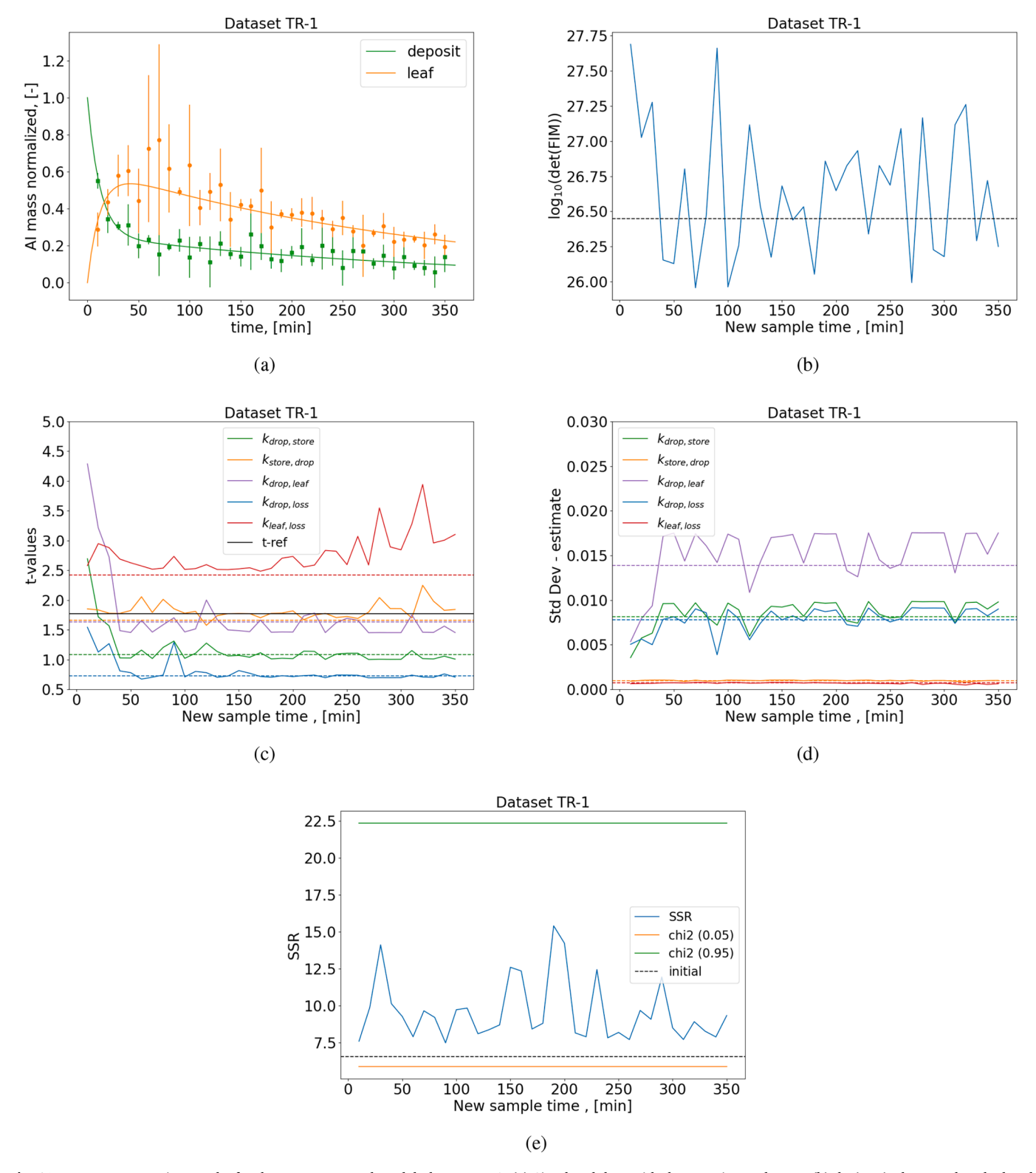


Fig. 10. Data augmentation results for the compartmental model, dataset TR-1. (a) Simulated data with the experimental error, (b) det(FIM) - log₁₀ scale calculated as in Eq. (5), (c) *t*-values, (d) standard deviation in the estimates, (e) SSR after data fitting. Dashed lines show the values obtained with the original dataset.

since the dataset dimensionality is small, just a single additional data point can have a significant impact. A similar oscillatory behaviour is observed also for the diffusion-based model.

The SSR increases for the compartmental model with the new data point, but it remains within the statistically significant region ($\chi^2_{0.05} - \chi^2_{0.95}$) in Fig. 10e. For the diffusion model, Fig. 11e, the quality of fitting

remains good from the statistical point of view and the SSR is slightly lower with the additional data point for most of the sampling times.

The quality of the estimates obtained with the new data is shown with the plots of *t*-test statistics and of the standard deviation of the estimates. These two profiles are related because the lower the parametric uncertainty, the higher the *t*-value, for a given estimate of the

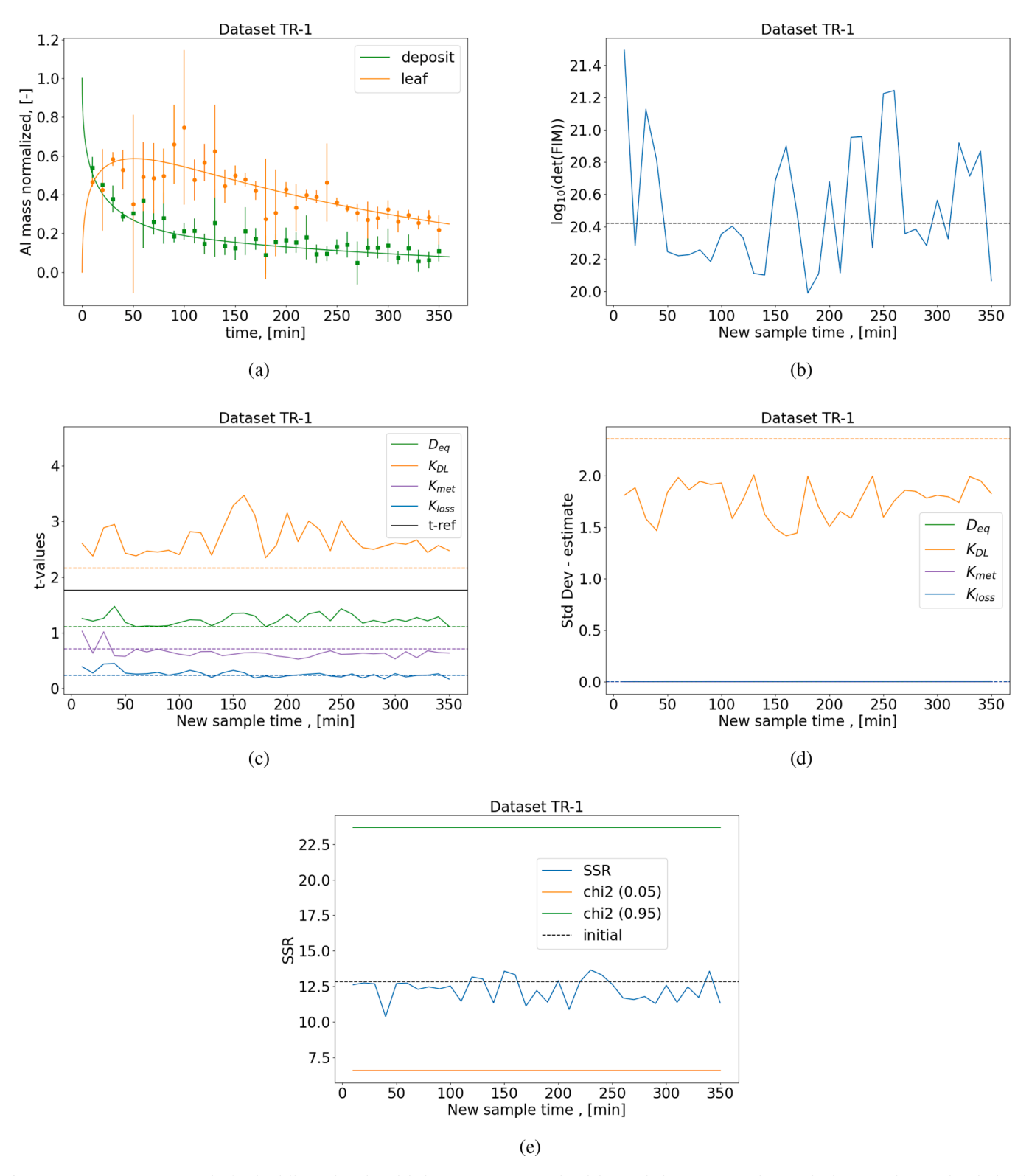


Fig. 11. Data augmentation results for the diffusion-based model, dataset TR-1. (a) Simulated data with the experimental error, (b) det(FIM) - log₁₀ scale calculated as in Eq. (5), (c) *t*-values, (d) standard deviation in the estimates, (e) SSR after data fitting. Dashed lines show the values obtained with the original dataset.

parameter, as per Eq. (10). For the compartmental model, adding a data point collected in the first 30 min can significantly improve the quality of the estimates, as shown in Fig. 10c, especially for the parameters $k_{drop,leaf}$, $k_{drop,store}$ and $k_{drop,loss}$, which were characterized by the lowest t-values. The early location in time of the most informative sample for these parameters is in agreement with the sensitivity profiles presented in Fig. 7.

The results obtained with the diffusion-based model are also in agreement with the sensitivity study shown in Fig. 8. For parameter K_{DL} , which was already estimated with good confidence, a general improvement in the quality of the estimate is observed with the additional experimental evidence. By analyzing the t-value for D_{eq} , a general improvement is observed as it approaches the reference t-value, suggesting that with some additional data it could be possible to further refine its

estimate. For parameters K_{met} and K_{loss} , which resulted to be strongly correlated from the previous analysis, the most informative samples are collected in the first 60 min as observed from the t-values in Fig. 11c, i.e. when the difference in their effect on the system dynamics is the maximum, however the quality of their estimate is still far from being statistically satisfactory.

4.3.2. Second augmented data study

The questions arising from the first data augmentation study in Section 4.3.1 are then: if more budget is potentially available to collect new samples from the same type of experiments, would it be possible to obtain a good estimation for these parameters? And if so, how many experiments would be required?

To answer these questions, the second data augmentation study described in the methodology (Section 2.2) is performed. This analysis is conducted only for the diffusion-based model since it is the only model with strongly correlated parameters. It is assumed to collect the new data in the time interval between 10 and 350 min, and to have a budget that goes up from 0 to 60 new data points equally spaced in this time frame.

Fig. 12 shows the results of the analysis for both datasets TR-1 and TR-2. For each case two plots are shown: i) one reporting the estimated values $\hat{\theta}$ and the respective standard deviation both normalized to the initial value of estimate, and ii) the *t*-value profiles plotted against the number of additional experimental points.

2.00

8 1.75

Pu 1.50

1.25

Pu 1.00

1.25

0.00

0 10 20 30 40 50 60

Number of additional samples

(a)

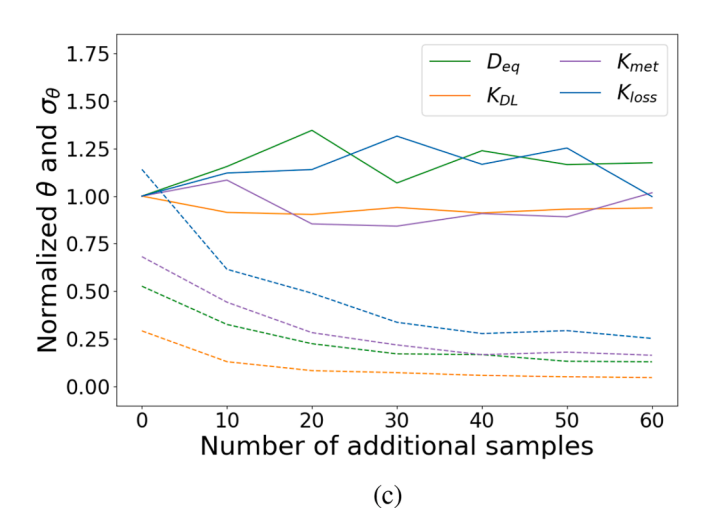
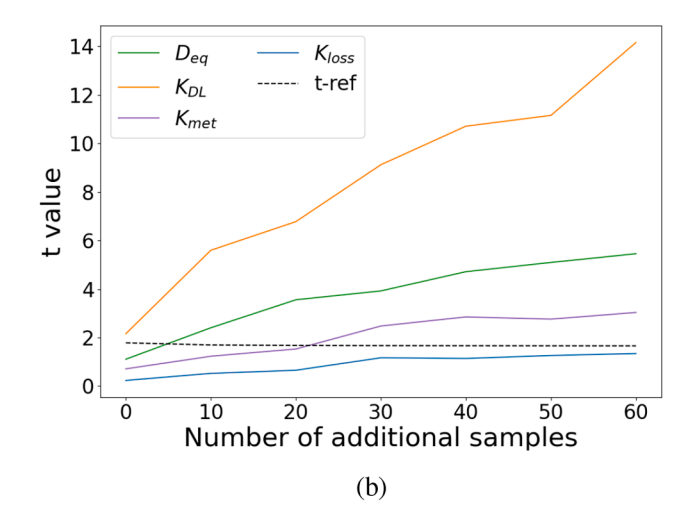


Table 3Correlation between the most critical parameter pairs in the data augmentation study. Initial value of correlation index (Init.), and correlation values observed with 10 to 60 additional samples.

Parameters	Data	Init.	10 s.	20 s.	30 s.	40 s.	50 s.	60 s.
$D_{eq} - K_{DL}$	TR-1	-0.77	-0.78	-0.72	-0.75	-0.87	-0.76	-0.72
$D_{eq} - K_{DL}$	TR-2	-0.89	-0.88	-0.85	-0.88	-0.93	-0.85	-0.87
$K_{met} - K_{loss}$	TR-1	-0.98	-0.98	-0.99	-0.99	-0.99	-0.99	-0.99
$K_{met} - K_{loss}$	TR-2	-0.97	-0.98	-0.99	-0.99	-0.98	-0.99	-0.98

It is interesting to observe that the uncertainty on all the four parameters D_{eq} , K_{DL} , K_{met} and K_{loss} drops significantly with the first 10 additional data points, and then keeps decreasing until 30 additional samples. After that point, the uncertainty keeps decreasing further, as shown by the increase in the t-values, but with a lower rate of improvement. The profiles of K_{met} and K_{loss} are of particular interest, being the two parameters strongly correlated. The t-value of K_{met} reaches the treference threshold after 20 additional samples are collected, both with dataset TR-1 and TR-2. Conversely, the initial uncertainty in K_{loss} varies significantly between TR-1 and TR-2, and this limits the capability in uncertainty reduction in the hypothetical scenario of pseudo-unlimited budget. As a consequence, its t-value after 30 additional samples is satisfactory for the case TR-2 but not for the case TR-1. Furthermore, as shown in Table 3 the strong correlation between K_{met} and K_{loss} is still



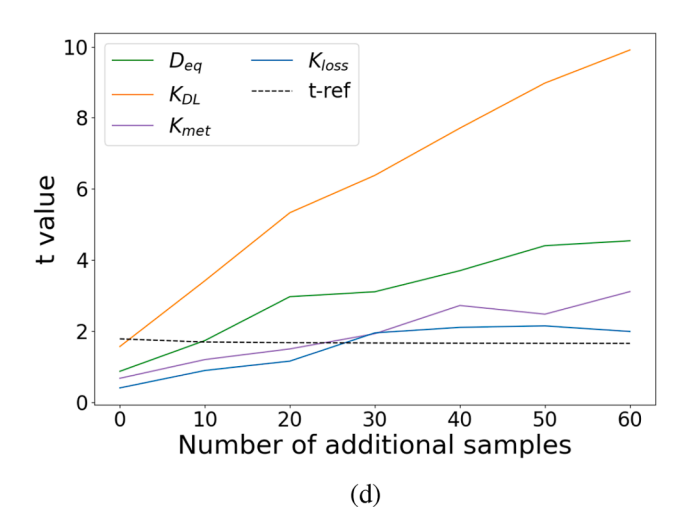


Fig. 12. Second data augmentation study: profiles of parameter estimates (solid lines) and standard deviations (dashed lines) normalized to the initial estimate, and profiles of the *t*-values against the number of additional samples with reference *t*-value (black dashed line). Datasets: (a), (b) TR-1; and (c), (d) TR-2.

present even with the new experimental information. These results confirm that K_{loss} is the most critical parameter to be estimated in the diffusion-based model if only this specific type of biokinetic experimental data is available.

This study can provide directions to the experimenters around what they should mostly look at before consuming experimental resources, which is the added value of combining computational research with the experimental work in this application. Still, this is a hypothetical study under the assumption of almost unlimited budget, but then considerations must be take into account on the actual experimental budget and practical feasibility of collecting that many samples in a short time period, not to mention that correlation issues are still present even in this theoretical scenario.

This analysis demonstrates that a number between 20 and 30 additional sampling points are needed to obtain statistically significant estimates for parameters K_{met} and K_{loss} , if the data are collected from this type of bio-kinetic experiments, and the correlation issues will still be present afterwards. If parameters can be decoupled, a good estimate could potentially be reached with a much lower number of samples, considering that collecting these many samples would be extremely expensive and time consuming, if not impractical. The modelers and experimentalists should then work together to evaluate other potential solutions, such as i) collecting data from different experiments that can allow an independent estimation of one of the two parameters, ii) correlate the problematic parameters to other physical and chemical properties of the crop-AI-formulation system, iii) reformulate the diffusion-based model. In terms of future directions, the possibility of using less but very precise samples will also be explored, combining it with a parametric study on the variance model for measurement errors.

5. Conclusions

This paper presented the application of a systematic modeling framework to understand and characterize the process of foliar uptake of pesticides. Different models have been considered, namely compartmental and diffusion-based models, and compared within the proposed modeling approach.

The study aims to develop a model that can be used in practice, together with the experimental observations, to extract more information about the system defined by crop-active ingredient-product formulation and potentially predict the expected uptake for new systems. To achieve this goal it is crucial to include practical considerations during all the steps of the modeling procedure, first of all ensure that model parameters are identifiable.

The analyses conducted in this paper focus on the concept of a-posteriori identifiability, which has been tested via dynamic sensitivity profiles and by studying the correlation between the parameters. An approach based on in silico data augmentation studies has been introduced in the modelling framework to study possible solutions to practical identifiability issues by collecting additional samples, while assessing the expected improvement in the estimates.

The parameters of the compartmental model are practically identifiable, even though some of them (i.e. $k_{drop,loss}$ and $k_{drop,store}$) are characterized by a large uncertainty in the preliminary estimate. The data augmentation study has demonstrated that their statistical quality can easily be improved by adding a few data points collected at the most informative sampling times.

In the diffusion-based model, the estimates of diffusion coefficient in the leaf, D_{eq} , and partition coefficient at the interface droplet-leaf, K_{DL} , can be improved with a limited number of additional samples, while the metabolic rate of AI consumption in the leaf, K_{met} , and the loss rate from the deposit K_{loss} are strongly correlated and an impractical number of additional samples, between 20 and 30, would be required to pass the statistical tests. To address this issue, a co-operation between modelers and experimentalists is advised to evaluate potential solutions, such as i) collecting data from different experiments that can allow an

independent estimation of one of the two parameters, ii) correlate the problematic parameters to other physical and chemical properties of the crop-AI-formulation system, iii) reformulate the diffusion-based model.

This study paves the way to further developments in the application of model-based design of experiments in a biological context characterized by high uncertainty in the experimental observations and in the model parameters. Further developments of the study will cover the uncertainty propagation from the model parameters to the predictions, coupled with the data augmentation study presented here. Another aspect that will be covered in future studies will be the impact of uncertainty in the initial conditions, i.e. the amount of AI initially present in the deposit, on model identification and how it would affect the model predictions. Finally, the application of model-based design of experiments (MBDoE) in foliar uptake experiments is also part of future works, considering the possibility of targeting uncertainty in model parameters, inputs, and model predictions, to validate the application of these techniques in a novel context.

CRediT authorship contribution statement

Enrico Sangoi: Writing – original draft, Writing – review & editing, Formal analysis, Investigation, Methodology, Conceptualization; Federica Cattani: Writing – review & editing, Methodology, Supervision, Conceptualization; Faheem Padia: Data curation; Federico Galvanin: Writing – review & editing, Methodology, Supervision, Conceptualization

Data availability

The data that has been used is confidential.

Declaration of competing interest

The authors declare that they have no known competing financial interests or personal relationships that could have appeared to influence the work reported in this paper.

Acknowledgments

The authors gratefully acknowledge the support of the Department of Chemical Engineering, University College London, UK and Syngenta.

Supplementary material

Supplementary material associated with this article can be found, in the online version, at 10.1016/j.ces.2025.121984.

References

Aktar, M.W., Sengupta, D., Chowdhury, A., 2009. Impact of pesticides use in agriculture: their benefits and hazards. Interdiscip. Toxicol. 2 (1), 1–12. https://doi.org/10.2478/v10102-009-0001-7

Bridges, R.C., Farrington, J.A., 1974. A compartmental computer model of foliar uptake of pesticides. Pestic. Sci. 5 (4), 365–381. https://doi.org/10.1002/ps.2780050402

Briggs, G.G., Rigitano, R. L.O., Bromilow, R.H., 1987. Physico-chemical factors affecting uptake by roots and translocation to shoots of weak acids in barley. Pestic. Sci. 19 (2), 101–112. https://doi.org/10.1002/ps.2780190203

Bronzato, M., Burriss, A., King, N., Donaldson, C., Sayer, D., Baker, C.M., 2023. Measuring the photostability of agrochemicals on leaves: understanding the balance between loss processes and foliar uptake. Pest Manag. Sci. 79, 3114–3121. https://doi.org/10.1002/ps.7488

Burkhardt, J., Basi, S., Pariyar, S., Hunsche, M., 2012. Stomatal penetration by aqueous solutions—An update involving leaf surface particles. New Phytol. 196 (3), 774–787. https://doi.org/10.1111/j.1469-8137.2012.04307.x

Fantke, P., Wieland, P., Wannaz, C., Friedrich, R., Jolliet, O., 2013. Dynamics of pesticide uptake into plants: from system functioning to parsimonious modeling. Environ. Model. Softw. 40, 316–324. https://doi.org/10.1016/j.envsoft.2012.09.016

- Fernández, V., Gil-Pelegrín, E., Eichert, T., 2021. Foliar water and solute absorption: an update. Plant J. 105 (4), 870–883. https://doi.org/10.1111/tpj.15090
- Forster, W.A., Zabkiewicz, J.A., Riederer, M., 2004. Mechanisms of cuticular uptake of xenobiotics into living plants: 1. Influence of xenobiotic dose on the uptake of three model compounds applied in the absence and presence of surfactants into Chenopodium album, Hedera helix and Stephanotis floribunda leaves. Pest Manag. Sci. 60 (11), 1105–1113. https://doi.org/10.1002/ps.918
- Franceschini, G., Macchietto, S., 2008. Model-based design of experiments for parameter precision: state of the art. Chem. Eng. Sci. 63 (19), 4846–4872. https://doi.org/10. 1016/j.ces.2007.11.034
- Franke, W., 1967. Mechanisms of foliar penetration of solutions. Annu. Rev. Plant Physiol. 18 (1), 281–300. https://doi.org/10.1146/annurev.pp.18.060167.001433
- Harris, C.R., Millman, K.J., van der Walt, S.J., Gommers, R., Virtanen, P., Cournapeau, D., Wieser, E., Taylor, J., Berg, S., Smith, N.J., Kern, R., Picus, M., Hoyer, S., van Kerkwijk, M.H., Brett, M., Haldane, A., Fernández del Río, J., Wiebe, M., Peterson, P., Gérard-Marchant, P., Sheppard, K., Reddy, T., Weckesser, W., Abbasi, H., Gohlke, C., Oliphant, T.E., 2020. Array programming with NumPy. Nature 585, 357–362. https://doi.org/10.1038/s41586-020-2649-2
- Li, Z., 2025. Plant uptake models of pesticides: advancing integrated pest management, food safety, and health risk assessment. Rev. Environ. Contam. Toxicol. 263 (1), 3. https://doi.org/10.1007/s44169-024-00076-y
- McKinney, W., et al., 2010. Data structures for statistical computing in Python. In: Proceedings of the 9th Python in Science Conference. Vol. 445. Austin, TX, pp. 51–56.
- Mercer, G.N., 2007. A simple diffusion model of the effect of droplet size and spread area on foliar uptake of hydrophilic compounds. Pestic. Biochem. Physiol. 88 (2), 128–133. https://doi.org/10.1016/j.pestbp.2006.10.004
- Miao, H., Xia, X., Perelson, A.S., Wu, H., 2011. On identifiability of nonlinear ODE models and applications in viral dynamics. SIAM Rev. 53 (1), 3–39. https://www.jstor.org/stable/41062109.
- Rodriguez-Fernandez, M., Egea, J.A., Banga, J.R., 2006. Novel metaheuristic for parameter estimation in nonlinear dynamic biological systems. BMC Bioinf. 7 (1), 483. https://doi.org/10.1186/1471-2105-7-483
- Rowland, M., Benet, L.Z., Graham, G.G., 1973. Clearance concepts in pharmacokinetics. J. Pharmacokinet. Biopharm. 1 (2), 123–136. https://doi.org/10.1007/BF01059626
- Sangoi, E., Cattani, F., Padia, F., Galvanin, F., 2024a. Foliar uptake models for biocides: testing practical identifiability of diffusion-based models. IFAC-PapersOnLine 58 (23), 73–78. https://doi.org/10.1016/j.ifacol.2024.10.013

- Sangoi, E., Cattani, F., Padia, F., Galvanin, F., 2024b. Foliar uptake models for biocides: testing structural and practical identifiability. Comput. Aided Chem. Eng. 53, 37–42. https://doi.org/10.1016/B978-0-443-28824-1.50007-7
- Satchivi, N.M., Stoller, E.W., Wax, L.M., Briskin, D.P., 2000. A nonlinear dynamic simulation model for xenobiotic transport and whole plant allocation following foliar application. I. Conceptual foundation for model development. Pestic. Biochem. Physiol. 68 (2), 67–84. https://doi.org/10.1006/pest.2000.2501
- Schreiber, L., 2006. Review of sorption and diffusion of lipophilic molecules in cuticular waxes and the effects of accelerators on solute mobilities. J. Exp. Bot. 57 (11), 2515–2523. https://www.istor.org/stable/24036240.
- Sharma, A., Kumar, V., Shahzad, B., Tanveer, M., Sidhu, G. P.S., Handa, N., Kohli, S.K., Yadav, P., Bali, A.S., Parihar, R.D., Dar, O.I., Singh, K., Jasrotia, S., Bakshi, P., Ramakrishnan, M., Kumar, S., Bhardwaj, R., Thukral, A.K., 2019. Worldwide pesticide usage and its impacts on ecosystem. SN Appl. Sci. 1 (11), 1446. https://doi.org/10.1007/s42452-019-1485-1
- Trapp, S., 2004. Plant uptake and transport models for neutral and ionic chemicals. Environ. Sci. Pollut. Res. 11 (1), 33–39. https://doi.org/10.1065/espr2003.08.169
- Tredenick, E.C., Farrell, T.W., Forster, W.A., Psaltis, S. T.P., 2017. Nonlinear porous diffusion modeling of hydrophilic ionic agrochemicals in astomatous plant cuticle aqueous pores: a mechanistic approach. Front. Plant Sci. 8, 746. https://doi.org/10.3389/fpls. 2017.00746
- Umetsu, N., Shirai, Y., 2020. Development of novel pesticides in the 21st century. J. Pestic. Sci. 45 (2), 54–74. https://doi.org/10.1584/jpestics.D20-201
- Virtanen, P., Gommers, R., Oliphant, T.E., Haberland, M., Reddy, T., Cournapeau, D., Burovski, E., Peterson, P., Weckesser, W., Bright, J., van der Walt, S.J., Brett, M., Wilson, J., Millman, K.J., Mayorov, N., Nelson, A. R.J., Jones, E., Kern, R., Larson, E., Carey, C.J., Polat, İ., Feng, Y., Moore, E.W., VanderPlas, J., Laxalde, D., Perktold, J., Cimrman, R., Henriksen, I., Quintero, E.A., Harris, C.R., Archibald, A.M., Ribeiro, A.H., Pedregosa, F., van Mulbregt, P., SciPy 1.0 Contributors, 2020. SciPy 1.0: fundamental algorithms for scientific computing in Python. Nat. Methods 17, 261–272. https://doi.org/10.1038/s41592-019-0686-2
- Walter, E., Pronzato, L., 1997. Identification of Parametric Models: From Experimental Data. Springer.
- Wieland, F.-G., Hauber, A.L., Rosenblatt, M., Tönsing, C., Timmer, J., 2021. On structural and practical identifiability. Curr. Opin. Syst. Biol. 25, 60–69. https://doi.org/10.1016/j.coisb.2021.03.005
- Zhang, Z.-Y., Ndikuryayo, F., Wang, J.-G., Yang, W.-C., 2025. How to identify pesticide targets? J. Agric. Food Chem. 73 (3), 1790–1800. https://doi.org/10.1021/acs.jafc.4c10080